RSC Advances

ROYAL SOCIETY OF CHEMISTRY

PAPER

View Article Online
View Journal | View Issue

Cite this: *RSC Adv.*, 2026, **16**, 15697

Unraveling the science of "sinking and dark-colored" superior agarwood through density, color, and metabolomics

Yanan Yuan,†[ac] Mengyuan Yang,†[bd] Yujiao Zhao[e] and Zhidong Qiu*[a]

Agarwood is a highly precious heartwood containing aromatic resin, which can be used both as medicine and incense. The consumption centers of agarwood are distributed worldwide, and many countries place great emphasis on the quality evaluation of agarwood. Throughout history, the appearance and physical characteristics of agarwood, such as sinkability and color, have often been used as indicators for quality assessment and commercial grading. However, the scientific basis of grading agarwood purely on appearance warrants additional exploration. In this study, 24 batches of agarwood were subjected to traditional sinkability tests and density measurements. The results revealed that samples floating wholly on the sea surface had densities ranging from 0.4465 to 0.7135, whereas samples partially or completely submerged had densities ranging from 0.5494 to 0.9075. Samples that sank completely to the bottom had densities above 1.0, confirming the consistency between sinkability and density. Using an intelligent visual analyzer, the appearance color of agarwood was digitally characterized. Combined with density results, it was found that as density increased, the overall *L**, *b** and *E***ab* values of agarwood gradually decreased, while the *a** values were consistently positive but relatively small. This indicates that agarwood tends to be dark red, and higher density correlates with darker color. UPLC-MS was employed to comprehensively analyze the chemical components of agarwood, leading to the identification of 89 compounds. Among them, 19 differential components were identified between agarwood with densities below 0.7 and those above 0.7. It was observed that agarwood with densities above 0.7 contained more chromone dimers, while those with densities below 0.7 contained more chromone monomers. This study validates the long-held idea that agarwood, which sinks in water and exhibits a darker color is of superior quality, revealing that such dense, sinking-grade agarwood is enriched with chromone dimers, which provide a scientific basis for its quality assessment.

Received 21st October 2025
Accepted 22nd February 2026

DOI: 10.1039/d5ra08081a

rsc.li/rsc-advances

1 Introduction

Agarwood is the resin-infused heartwood formed in members of the genus *Aquilaria* (family Thymelaeaceae) as a response to wound-induced defense mechanisms. *Aquilaria sinensis* is native to regions of China, including Guangdong, Hainan, Guangxi, and Fujian, and is also distributed in countries such as Indonesia, Vietnam, and Malaysia.[1] Owing to its resource scarcity and high market value, agarwood is considered one of the most precious woods globally. It is often stated that "one tael of agarwood is worth one tael of gold", underscoring its exceptional status.[2,3] Historical records from the Famen Temple site of the Tang Dynasty indicate that agarwood was offered by the imperial family as a key aromatic offering to the Buddha's finger relic.[4] Furthermore, the renowned Song Dynasty painting *Along the River During the Qingming Festival* depicts shops engaged in agarwood trade (Fig. S1A). Beyond its cultural significance, agarwood is widely utilized in various fields, including perfumery, incense, fragrances, and traditional medicine, due to the distinctive scent of its resin.[2]

In market transactions, agarwood is classified into different commercial grades based on empirical identification. These traditional assessment criteria primarily include sensory and physical characteristics such as sinkability, aroma, color, and resin content.[5] The Chinese term for agarwood, "Chenxiang", is highly descriptive; the word "Chen" denotes its ability to sink in water, indicating high density. Similarly, in Malaysia and Indonesia, grading standards also emphasize appearance, where a darker color and higher density are generally indicative of a superior grade.[6] The Qing Dynasty pharmacopeia Ben Cao Qiu Zhen (AD 1769) systematically

[a]*Changchun University of Chinese Medicine, Changchun 130117, China*
[b]*State Key Laboratory for Quality Ensurance and Sustainable Use of Dao-di Herbs, National Resource Center for Chinese Materia Medica, China Academy of Chinese Medical Sciences, Beijing 100700, China*
[c]*China Academy of Chinese Medical Sciences, Beijing 100700, China*
[d]*Key Scientific Research Base of Traditional Chinese Medicine Heritage (Institute of Chinese Materia Medica, China Academy of Chinese Medical Sciences), National Cultural Heritage Administration, Beijing, 100700, P. R. China*
[e]*College of Pharmacy, Anhui University of Chinese Medicine, Hefei 230012, China*
† Yanan Yuan and Mengyuan Yang contributed equally to this work.

summarized the criteria for premium agarwood: a black color, a solid texture, and the ability to sink in water (Fig. S1B).

Modern chemical studies have revealed that the aromatic resin in agarwood is a class of secondary metabolites produced by *Aquilaria* plants in response to physical or chemical injury to initiate defense mechanisms. Its primary constituents are sesquiterpenes and 2-(2-phenylethyl)chromones (PECs).[7] Among them, 2-(2-phenylethyl)chromones (PECs), as a major class of chemical components in agarwood, not only contribute to its distinctive aroma but also possess various pharmacological activities, serving as the key material basis for both its medicinal efficacy and aromatic properties. These components are often used as critical indicators for evaluating agarwood quality.[8] For instance, the current *Chinese Pharmacopoeia* specifies the content of agarotetrol (a specific PEC) as an indicator for quality control.[9] Meng Yu reported a notably greater abundance of 2-(2-phenylethyl)chromone and 2-[2-(4-methoxyphenyl)ethyl]chromone in high-quality wild Chi-Nan agarwood than in ordinary agarwood.[10] Lin Wanting proposed that quality assessment of agarwood requires comprehensive consideration of differences in morphological characteristics, chemical composition, and biological activity, advocating for an evaluation based on integrated analytical results.[11] Fu Yuejin *et al.*, in a study of 223 agarwood samples of varying origins and qualities, suggested that evaluation based on sensory characteristics such as appearance and aroma possesses a degree of scientific validity. They further indicated that the sum of the relative contents of the ethanol extract, 2-[2-(4-methoxyphenyl)ethyl]chromone, and 2-(2-phenylethyl)chromone also serves as an important criterion for grading agarwood quality.[12] However, the correlation between traditional empirical identification and the chemical composition of agarwood still lacks systematic modern scientific validation.

This study conducted traditional sinkability tests, determination of ethanol extract, and density measurements on 24 batches of collected agarwood. Intelligent visual analysis and UPLC-MS were employed to determine their color parameters and chemical composition, respectively. This approach aims to systematically investigate the correlation between traditional empirical assessments and chemical constituents, thereby laying a foundation for quality grading of agarwood.

2 Experimental part

2.1 Chemicals and materials

Agarotetrol (Batch No. PS011165, purity ≥ 98%), 8-chloro-5,6,7-trihydroxy-2-(2-phenylethyl)tetrahydrochromone (Batch No. PS013241, purity ≥ 98%), 6,7-dimethoxy-2-(2-phenylethyl) chromone (Batch No. PS011187, purity ≥ 98%), 6,7-dihydroxy-2-(2-phenylethyl)-5,6,7,8-tetrahydrochromone (Batch No. PS013272, purity > 98%), (5S,6R,7S,8R)-2-(2-phenylethyl)-5,6,7-trihydroxy-5,6,7,8-tetrahydro-8-[2-(2-phenylethyl)chromon-6-yloxy]chromone (Batch No. PS013323, purity > 95%), and (5R,6R,7R,8S)-2-(2-phenylethyl)-5,6,7-trihydroxy-5,6,7,8-tetrahydro-8-[2-(2-phenylethyl)chromon-6-yloxy]chromone (Batch No. PS013322, purity > 95%) were all purchased from Chengdu Push Bio-technology Co.,Ltd (Chengdu, Sichuan, China). Isoagarotetrol (Batch No. AZDH0202, purity: 98%), 2-(2-phenylethyl)chromone (Batch No. AZDD0305, purity: 98%), 6-methoxy-2-(2-phenylethyl)chromone (Batch No. AFCH0403, purity: 98%), 6,7-dimethoxy-2-[2-(4-hydroxyphenyl)ethyl] chromone (Batch No. AZEB2012, purity: 98%), 6-methoxy-2-[2-(3-methoxyphenyl)ethyl]chromone (Batch No. AFDI3002, purity: 98%), 6-hydroxy-2-(2-phenylethyl)chromone (Batch No. AFCB2104, purity: 98%), 6,7-dimethoxy-2-[2-(4-hydroxyphenyl) vinyl]chromone (Batch No. AZEB2011, purity: 98%), 4′-methoxyisoagarotetrol (Batch No. AFDI3001, purity: 98%), and 4′-methoxyagarotetrol (Batch No. AFDB2201, purity: 98%) were all purchased from Chengdu Alfa Biotechnology Co., Ltd (Chengdu, Sichuan, China). 6,7-Dimethoxy-2-[2-(4-methoxyphenyl)ethyl]chromone (Batch No. 15968-G250401, purity ≥ 8%) was purchased from the Shanghai Standard Technology Service Co., Ltd (Shanghai, China); 2-[(4-methoxyphenyl)ethyl]chromone was purchased from the Chinese Academy of Tropical Agricultural Sciences (Haikou, Hainan, China). Methanol, acetonitrile, and formic acid, all of chromatographic grade, were used in this study.

A total of 24 batches of agarwood samples of different specifications were procured from the Dianbai Agarwood Market (Maoming, Guangdong Province, China) in 2024 (Fig. 1). All samples were identified by Prof. Peng Huasheng (China Academy of Chinese Medical Sciences) as originating from *Aquilaria sinensis* (Lour.) Spreng.

2.2 Determination of ethanol extract of agarwood

A 2.0 g sample of agarwood powder (denoted as M_0) was accurately weighed into a 100 mL conical flask. Subsequently, 50 mL

Fig. 1 Sample images of twenty-four lots of agarwood. Labels (a–x) correspond to agarwood samples CX001–CX024, Scale bar = 2 cm.

of anhydrous ethanol was precisely added to the flask, and the total mass was recorded. After standing at room temperature for 1 hour, the mixture was heated under reflux for 1 hour, maintaining a state of gentle boiling. Following cooling to room temperature, the total mass was recorded again, and any mass loss due to evaporation was compensated by the addition of anhydrous ethanol. The mixture was then filtered. A precise 25 mL aliquot of the filtrate was transferred to a pre-dried and pre-weighed evaporation dish (constant mass denoted as M_1). The solvent was evaporated to dryness on a water bath. The residue was further dried in an oven at 105 °C for 3 hours, cooled in a desiccator for 30 minutes, and immediately weighed accurately (denoted as M_2). The content of the ethanol-soluble extractives was calculated according to the formula provided below:

$$\text{Ethanol extract content } (\%) = \frac{((M_2 - M_1) \times 2)}{M_0} \times 100\%$$

2.3 Sinkability test and density measurement of agarwood

The sinkability test was performed by placing the agarwood sample into a beaker containing 1500 mL of pure water. After allowing it to stand for 2 minutes to stabilize its position, the final location of the sample in the water was observed and recorded.

For density measurement, the agarwood block was first left in the testing environment for 30 minutes, and its mass was weighed and recorded as M_1 (dry mass). A beaker filled with sufficient distilled water to submerge the sample was placed on an electronic balance. The sample was then fixed with a thin line and a fine needle and completely immersed in the water. The reading on the balance was monitored, and once stabilized, the sample was removed. Its mass was immediately weighed and recorded as M_2, representing the mass of the sample in a relatively water-saturated state. Next, the beaker containing distilled water was placed back on the electronic balance, and the reading was tared to zero. The sample was immersed again, and the stable value displayed by the balance was recorded as M_3, representing the mass of water displaced by the sample (equivalent to the buoyant force according to Archimedes' principle). For each batch of agarwood, no fewer than three replicate samples were subjected to parallel density determinations. The density (ρ) of each agarwood sample was calculated using the following formula:

$$\rho = \frac{M_1}{M_3 - (M_2 - M_1)} \times \rho_{\text{water}}$$

2.4 Color analysis of agarwood by smart visual analysis

Color measurement was performed using a VA400 IRIS visual analyzer. After powering on the instrument and allowing it to stabilize (indicated by a green light), calibration was conducted using a 24-color calibration plate. The lens exposure and focal length were adjusted to optimal settings. Images were captured using both top and bottom illumination in a single snapshot mode. Agarwood samples from different batches were ground and passed through a No. 3 sieve. The resulting powder was evenly spread in a clean Petri dish. Color images of the samples were then acquired using the visual analyzer, with each sample measured in triplicate. The color parameters collected and calculated for each agarwood sample included the lightness (L^*), green–red value (a^*), blue–yellow value (b^*), and total chromaticity value (E^*ab). The E^*ab value was determined using the following formula:

$$E^*ab = [(L^*)^2 + (a^*)^2 + (b^*)^2]^{1/2}$$

2.5 UPLC-Q-TOF-MS analysis

2.5.1 Preparation of mixed standard solution. Individual reference standards, including agarotetrol, isoagarotetrol, 4′-methoxyagarotetrol, 4′-methoxyisoagarotetrol, 6,7-dihydroxy-2-(2-phenylethyl)-5,6,7,8-tetrahydrochromone, 6,7-dimethoxy-2-[2-(4-hydroxyphenyl)ethyl]chromone, 6,7-dimethoxy-2-[2-(4-hydroxyphenyl)vinyl]chromone, 8-chloro-5,6,7-trihydroxy-2-(2-phenylethyl)-5,6,7,8-tetrahydrochromone, 6-hydroxy-2-(2-phenylethyl)chromone, 6,7-dimethoxy-2-[2-(4-methoxyphenyl) ethyl]chromone, 6,7-dimethoxy-2-(2-phenylethyl)chromone, 2-(2-phenylethyl)chromone, 2-[(4-methoxyphenyl)ethyl] chromone, 6-methoxy-2-(2-phenylethyl)chromone, 6-methoxy-2-[2-(3-methoxyphenyl)ethyl]chromone, (5R,6R,7R,8S)-2-(2-phenylethyl)-5,6,7-trihydroxy-5,6,7,8-tetrahydro-8-[2-(2-phenylethyl)chromon-6-yloxy]chromone, and (5S,6R,7S,8R)-2-(2-phenylethyl)-5,6,7-trihydroxy-5,6,7,8-tetrahydro-8-[2-(2-phenylethyl)chromon-6-yloxy]chromone, were accurately weighed (approximately 3 mg each). These were then dissolved and diluted with ethanol to prepare a mixed standard working solution with a concentration of approximately 100 μg mL^{-1} for each component.

2.5.2 Preparation of test solution. A quantity of 0.1 g of agarwood powder (passed through a No. 3 sieve) was accurately weighed and transferred into a stoppered conical flask. Then, 10 mL of ethanol was precisely added, and the total weight was recorded. After soaking for 0.5 hours, the mixture was subjected to ultrasonic extraction for 1 hour. Following extraction, the solution was cooled to room temperature, and the total weight was measured again. Any weight loss was compensated by adding ethanol. The mixture was shaken thoroughly, allowed to stand, and the supernatant was then passed through a 0.22 μm microporous membrane. The subsequent filtrate was collected as the final test solution.

2.5.3 Preparation of quality control (QC) sample. A 1 mL aliquot of the test solution from each agarwood sample was combined and thoroughly mixed. The resulting pooled solution was filtered through a 0.22 μm microporous membrane, and the subsequent filtrate was collected as the quality control (QC) sample. To evaluate the reliability of the analytical method, the QC sample was injected six times at the beginning of the analytical sequence (1 μL per injection). Subsequently, it was injected once every four test samples throughout the sequence. The reliability of the analytical method was assessed by calculating the relative standard deviation (RSD) of the retention time for each reference substance in the QC samples (all < 0.28%), as well as by evaluating the tight clustering of the QC samples in the principal component analysis (PCA).

2.5.4 UPLC-Q-TOF-MS condition

2.5.4.1 Chromatographic conditions. Separation was achieved using a Waters Acquity UPLC ® HSST3 C_{18} column (2.1 × 100 mm, 1.8 μm). The mobile phase consisted of acetonitrile (A) and 0.1% formic acid in water (B), delivered at a flow rate of 0.3 mL min^{-1}. The gradient elution program was set as follows: 0–5 min, 18% A; 5–10 min, 18–30% A; 10–28 min, 30–50% A; 28–33 min, 50–85% A; 33–35 min, 85% A. The column temperature was maintained at 30 °C, the sample compartment temperature was set at 10 °C, and the injection volume was 1 μL.

2.5.4.2 Mass spectrometric conditions. Analysis was performed on an Xevo G2-XS Q-TOF mass spectrometer. The mass scan range was set to *m*/*z* 50–1500 Da. The drying gas (N_2) flow rate was 800 L h^{-1} at a temperature of 450 °C. The ionization source temperature was 120 °C. The cone gas flow rate was 50 L h^{-1} with a cone voltage of 40 V. The capillary voltage was set to +3.0 kV for positive mode and −2.5 kV for negative mode. In MSE mode, the low collision energy was 6 V, and the high collision energy was ramped from 15–50 V. Data were acquired in both positive and negative electrospray ionization (ESI) modes. A leucine-enkephalin solution (200 pg μL^{-1}) was used as the lock mass reference for real-time mass calibration, infused at a flow rate of 5 μL min^{-1}, generating reference ions at *m*/*z* 556.2771 $[M + H]^+$ in positive mode and *m*/*z* 554.2615 $[M - H]^-$ in negative mode.

2.5.5 Data processing. The raw data acquired from UPLC-Q-TOF-MS were processed using Masslynx software. Possible elemental compositions were calculated based on the accurate molecular masses, with candidate molecular formulas selected within an error tolerance of ±3 mDa. Compound identification was subsequently performed by comparing data against available reference standards, retention times, accurate mass measurements from MS spectra, and characteristic fragment ions from MS/MS spectra, supplemented by consultations with relevant literature reports.

The raw data acquired from UPLC-Q-TOF-MS were imported into Progenesis QI software for preprocessing, which included peak picking, peak alignment, and normalization. This procedure ultimately generated a data matrix comprising retention time, *m*/*z*, and normalized abundance. The resulting data matrix was then imported into SIMCA 14.1 software for multivariate data analysis. Principal component analysis (PCA) and orthogonal partial least squares-discriminant analysis (OPLS-DA) were performed. Differential ions were screened based on the criteria of a variable importance in projection VIP > 1, $p < 0.05$, and a max fold change either < 0.5 or > 2.

2.6 UPLC-QQQ-MS

2.6.1 Preparation of mixed standard solution. Accurate quantities of 2-(2-phenylethyl)chromone, 2-[(4-methoxyphenyl)ethyl]chromone, 6-methoxy-2-(2-phenylethyl)chromone, and 6,7-dimethoxy-2-[2-(4-hydroxyphenyl)ethyl]chromone were weighed and dissolved in methanol to prepare individual stock solutions with mass concentrations of 4.04 mg mL^{-1}, 6.29 mg mL^{-1}, 1.81 mg mL^{-1}, and 2.61 mg mL^{-1}, respectively.

Each stock solution was subsequently diluted 10 000-fold to prepare 200 ng mL^{-1} working solutions for optimizing mass spectrometry parameters.

For the linearity investigation, a 100 μL aliquot from each stock solution was transferred to a single 10 mL volumetric flask. The mixture was brought to volume with methanol, creating a mixed reference standard solution containing the four compounds. This mixed solution was then serially diluted to prepare working solutions at varying concentrations for establishing calibration curves.

2.6.2 Preparation of test solution. Exactly 25 mg of agarwood powder was accurately weighed and transferred into a 50 mL volumetric flask. The flask was filled to the mark with chromatographic-grade methanol and the total weight was recorded. After soaking for 0.5 h, the mixture was subjected to ultrasonic extraction for 1 h. The solution was then cooled to room temperature, reweighed, and any weight loss was compensated by adding methanol. After thorough mixing, the supernatant was filtered through a 0.22 μm microporous membrane to obtain the final test solution.

2.6.3 UPLC-QQQ-MS condition

2.6.3.1 Chromatographic conditions. Separation was performed on a Waters 186002352 ACQUITY UPLC ® BEH C_{18} column (2.1 × 100 mm, 1.7 μm). The mobile phase consisted of 0.5% formic acid in water (A) and acetonitrile (B) with a gradient elution program set as follows: 0–1 min, 16% ∼17% B; 1–5 min, 17% ∼19% B; 5–10 min, 19% ∼48% B; 10–19 min, 48% ∼80% B; 19–20 min, 80% ∼100% B; 20–35 min, 100% B. The injection volume was 1 μL, the flow rate was maintained at 0.3 mL min^{-1}, and the column temperature was set at 40 °C.

2.6.3.2 Mass spectrometric conditions. Analysis was carried out using an electrospray ionization (ESI) source in positive ion mode with full scan detection. The ion source parameters were set as follows: ion spray voltage, 5500 V; turbo heater temperature, 500 °C; curtain gas (CUR), 30 psi; ion source gas 1 (GS1, nebulizer gas), 50 psi; and ion source gas 2 (GS2, auxiliary gas), 50 psi. The mass spectrometry parameters and retention times for the four chromone components are listed in Table 1.

The extracted ion chromatograms of the four constituents in the mixed reference standard solution and the test solution are shown in Fig. 2. The retention times of each component in the mixed standard solution were consistent with those of the corresponding compounds in the test solution.

2.6.4 Method validation. Mixed reference standard solutions at seven different concentration levels for each compound were analyzed by LC-MS. The peak area of each reference standard at different concentrations was recorded. Using the mass concentration (X) of the reference standard as the abscissa and the corresponding peak area (Y) as the ordinate, linear regression was performed to obtain the linear regression equation and correlation coefficient (r) for each compound. The mixed reference standard solution was injected six times consecutively. The peak areas of the four components were recorded, and the relative standard deviation (RSD) was calculated. The test solution was analyzed at 0, 2, 4, 8, 12, and 24 hours. The peak areas of the four components at these different time points were recorded, and the RSD was calculated to

Table 1 Mass spectrometric parameters of the four analytes

Compound	RT (min)	Q1 (*m*/*z*)	Q2 (*m*/*z*)	DP (V)	CE (V)
2-(2-Phenylethyl)chromone	13.56	251.1	160.2	115	33.85
2-[(4-Methoxyphenyl)ethyl]chromone	13.31	281.0	121.2	100	31.00
6-Methoxy-2-(2-phenylethyl)chromone	14.02	281.0	190.1	130	36.00
6,7-Dimethoxy-2-[2-(4-hydroxyphenyl)ethyl]chromone	10.41	327.1	221.1	140	21.00

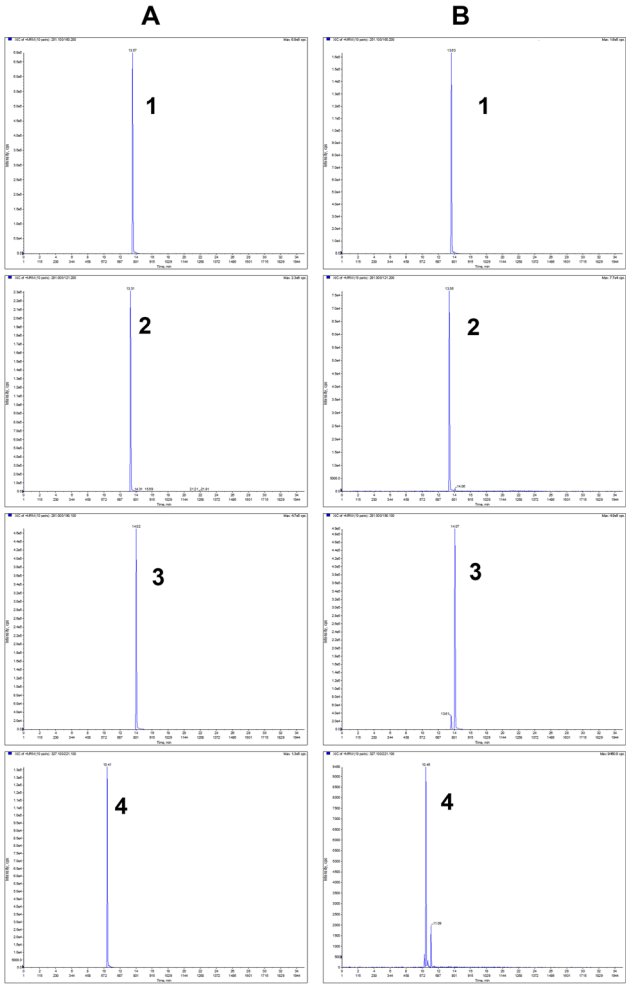

Fig. 2 Extracted ion chromatograms (EICs) of the four analytes in the mixed reference standard solution and the test solution. (A) Represents the mixed reference standard solution; (B) represents the test solution. Peak 1: 2-(2-phenylethyl)chromone; peak 2: 2-[(4-methoxyphenyl) ethyl]chromone; peak 3: 6-methoxy-2-(2-phenylethyl)chromone; peak 4: 6,7-dimethoxy-2-[2-(4-hydroxyphenyl)ethyl]chromone.

evaluate the stability of the solution. Six parallel test solutions were prepared independently. The content of each of the four components in the crude drug was calculated using their respective linear regression equations, and the RSD of the content values was calculated. Six portions of a known-content agarwood sample powder (12.5 mg each) were accurately weighed. A precise volume of the mixed reference standard stock solution was added to each portion, such that the amount of each added standard was approximately equal to the original amount of the corresponding analyte present in the sample (a 1 : 1 ratio). The spiked samples were then analyzed, and the peak areas were recorded. The recovery rate was calculated using the following formula:

$$\text{Recovery } (\%) = (M_1 - M_2)/M_3 \times 100\%$$

M_1 is the measured total amount, M_2 is the original content of the analyte in the sample, and M_3 is the amount of the reference standard added.

3 Results and discussion

3.1 Relationship between sinkability, density and ethanol extract content of agarwood

Based on their buoyancy behavior in water, the 24 batches of agarwood were classified into three categories (Table 2): non-sinking (9 batches), partially sinking (9 batches), and completely sinking (6 batches). Analysis of the density values for each batch (Fig. 3) revealed that the nine non-sinking samples exhibited densities ranging from 0.4465 to 0.7135, while the nine partially sinking samples showed densities between 0.5494 and 0.9075. All 6 completely sinking samples possessed densities greater than 1.0. The density ranges overlapped between the non-sinking and slightly sinking groups, which could be attributable to the agarwood's heterogeneous resin distribution. Furthermore, for agarwood samples with similar densities, the traditional sinkability test results may be influenced by factors such as water temperature, water purity, sample geometry, and the presence of trapped air within internal pores, potentially resulting in unstable or inaccurate assessments. Overall, a strong consistency was observed between the sinking behavior determined by the traditional test and the measured density values. Based on the integrated results of the sinkability test and density measurements, a classification system can be established: samples with densities ranging from 0.4 to 0.7 are categorized as non-sinking, those with densities between 0.7 and 1.0 as partially sinking, and those with densities greater than 1.0 as completely sinking.

As a core indicator for assessing agarwood quality, the ethanol-soluble extract content is widely used as a representative measure of its resin content.[13] In this study, a total of 24 batches of agarwood with varying specifications were collected. Due to insufficient sample quantity for batch CX024, the ethanol-soluble extract content was determined for the remaining 23 batches (CX001–CX023) to investigate the relationship between sinking behavior, density, and resin content (Table 2). As shown in Fig. 3, sinking-grade agarwood with

Table 2 Sinking property, ethanol extract content and density range of twenty-four lots of agarwood

ID number	Specification	Sinking property	Density value (mean ± SD, $n \geq 3$)	Density range	Ethanol extract content (%)	Ethanol extract range (%)
CX001	Stump (white-fiber)	Non-sinking	0.5370 ± 0.1308	0.4465–0.7135	18.20	15.17–37.67
CX002	Stump (rubbed-head grade C)		0.5731 ± 0.0287		17.24	
CX003	Stump (aged-head grade B)		0.7101 ± 0.0090		22.07	
CX004	Bug-hole agarwood grade A		0.5366 ± 0.0158		27.31	
CX005	Gash agarwood		0.4856 ± 0.0551		15.17	
CX006	Water-grained agarwood		0.4465 ± 0.0459		22.69	
CX018	Hainan capped-head agarwood		0.7135 ± 0.1282		25.20	
CX020	Hainan aged-head (select)		0.6501 ± 0.0444		37.67	
CX022	Earth-aged bug-hole agarwood		0.5265 ± 0.0886		21.64	
CX007	Bark-oil agarwood grade C	Partial-sinking	0.6495 ± 0.1249	0.5494–0.9075	26.16	17.56–44.01
CX008	Bark-oil agarwood grade B		0.8435 ± 0.0383		31.65	
CX009	Saw-marked agarwood		0.8073 ± 0.0839		44.01	
CX010	Shell agarwood grade B		0.7709 ± 0.1220		31.42	
CX011	Deadwood agarwood		0.8158 ± 0.0548		36.73	
CX012	Spreading-oil agarwood		0.5494 ± 0.0924		20.68	
CX013	Iron-head (capped)		0.8067 ± 0.0650		23.82	
CX014	Earth-aged agarwood		0.6052 ± 0.0443		17.56	
CX021	Saw-cut agarwood (select)		0.9075 ± 0.0434		35.00	
CX015	Capped-head (type 1–2)	Sinking	1.1763 ± 0.02959	1.0547–1.1763	41.05	32.12–62.59
CX016	Capped-head (type 1–3)		1.0574 ± 0.0441		62.59	
CX017	Bark-oil agarwood grade A		1.0453 ± 0.0171		32.12	
CX019	Sinking aged capped-shell		1.1237 ± 0.0875		32.29	
CX023	Sinking bug-hole agarwood (select)		1.0725 ± 0.0458		44.18	
CX024	Chinese sinking agarwood		1.0547 ± 0.7900		—	

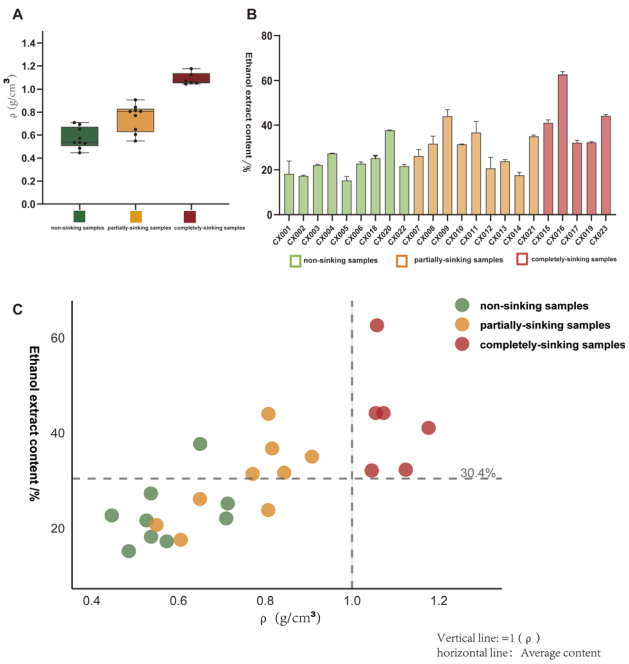

Fig. 3 Relationship between sinkability, density and ethanol extract content of agarwood. (A) Relationship between sinkability and density value; (B) relationship between sinkability and ethanol extract content; (C) relationship diagram of sinkability, density and ethanol extract content.

higher density exhibited significantly greater resin content compared to non-sinking and partially sinking grades, demonstrating a positive correlation between the sinking property and resin content in agarwood. Additionally, no distinct difference in resin content was observed between the non-sinking and partially sinking groups, which may be attributed to the uneven distribution of resin within the wood tissue.

In China, agarwood has historically been recognized with the adage "sinking in water indicates superior quality". The sinkability of agarwood serves as a comprehensive external manifestation of resin accumulation during its formation process. It is widely held that agarwood blocks floating on the water surface possess low resin content and are thus considered inferior products.[6] Furthermore, the market price of agarwood is primarily determined by its quality. Currently, the grading of commercial agarwood still largely relies on empirical identification. Notably, for the 24 batches of agarwood samples collected in this study, a strong correlation was observed between market price and experimentally measured density: the partially sinking samples (particularly those with higher density) generally commanded higher market prices than the non-sinking ones (with lower density); meanwhile, the completely sinking samples (with higher density) were consistently priced higher than both the partially sinking and non-sinking samples.

3.2 Linking color to density in agarwood

The color of powdered agarwood samples was measured using an intelligent visual analyzer. The collected and calculated color parameters for each sample included the lightness (L^*), green–red value (a^*), blue–yellow value (b^*), and total chromaticity value (E^*ab). The L^* value ranges from 0 to 100, representing

a transition from black to white. A positive to negative scale for the a^* value indicates a color shift from red to green, while a similar scale for the b^* value denotes a transition from yellow to blue. The E^*ab value, representing the total chromaticity of each sample, correlates with color intensity; a higher E^*ab value indicates a lighter color.

Based on their density, the 24 batches of agarwood samples were divided into three groups: Group A (density 0.4–0.7), Group B (density 0.7–1.0), and Group C (density > 1.0). The results of the lightness (L^*) values for each group showed that Group A samples had L^* values ranging from 51.0776 to 66.4042, Group B ranged from 50.4976 to 64.0695, and Group C ranged from 38.4019 to 57.9143. As shown in Fig. 4A, the overall L^* value of agarwood gradually decreased with increasing density, indicating that samples with higher density exhibited darker coloration.

The results for the red–green value (a^*) across the different groups showed that Group A agarwood samples had a^* values ranging from 3.6520 to 8.0938, Group B ranged from 5.1811 to 8.0159, and Group C ranged from 3.8306 to 7.8404. As shown in Fig. 4B, the a^* value did not exhibit a significant change with increasing density. The a^* values for all groups were consistently positive and remained below 8.0938, indicating a dark reddish hue in agarwood samples across different density grades.

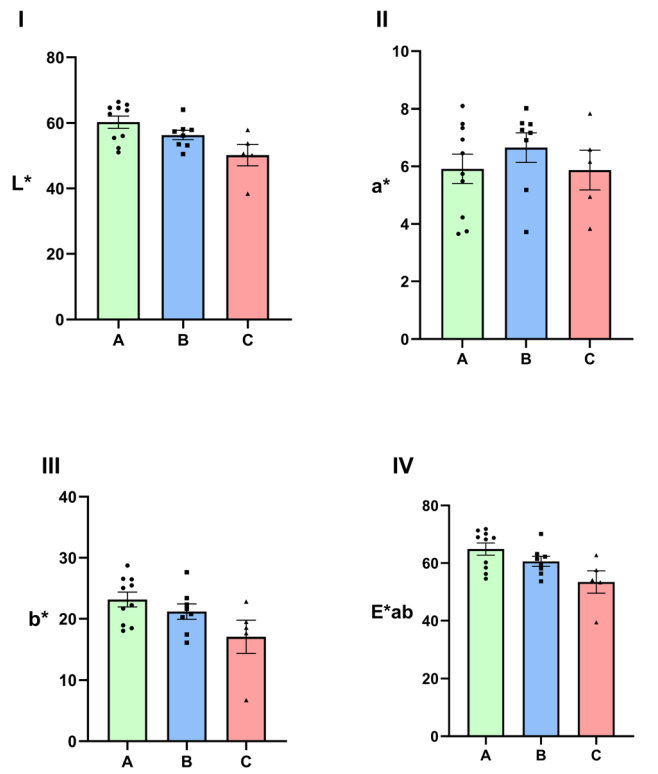

Fig. 4 Lightness value (L^*), red–green value (a^*), yellow–blue value (b^*) and total chromaticity value (E^*ab) of each group of agarwood samples. (I) shows the lightness value (L^*) of each group of agarwood samples; (II) shows the red–green values (a^*) of each group of agarwood samples; (III) shows the yellow–blue value (b^*) of each group of agarwood samples and (IV) shows the total chromaticity value (E^*ab) of each group of agarwood samples.

The results for the blue–yellow value (b^*) across the sample groups demonstrated that Group A exhibited b^* values ranging from 18.0543 to 28.7385, Group B from 16.0892 to 27.6386, and Group C from 6.7452 to 22.8323. As illustrated in Fig. 4C, the b^* values for all groups were positive, and a gradual decrease in the overall b^* value of agarwood was observed with increasing density. This indicates a reduction in the yellow tone of the samples as density rises.

Regarding the total chromaticity value (E^*ab), the results showed E^*ab values of 54.5971–71.8553 for Group A, 53.6686–70.1442 for Group B, and 39.4739–62.7444 for Group C. Fig. 4D reveals a progressive decline in the E^*ab value of agarwood with increasing density, demonstrating that the overall color of the wood deepens as it becomes denser.

In the assessment of agarwood, color evaluation serves as one of the important criteria for determining its quality.[6] However, traditional visual identification is susceptible to influences from lighting conditions and subjective experience. The smart visual analyzer enables more precise discrimination by quantifying color parameters, thereby enhancing the scientific rigor, objectivity, and efficiency of the evaluation. This aligns with records in the ancient Chinese herbal text Yaoxing Yaolue Daquan (AD 1545), which states, "The best quality is that which sinks in water, has a firm and solid texture, and is dark in color", indicating that dark, sinkable agarwood is of superior quality. When agarwood exhibits a brown or dark coloration, its resin content and quality are generally considered to be relatively high.[14] As noted by Rozi Mohamed and Shiou Yih Lee, the density and color of agarwood are regarded as key indicators of high-quality material, with darker-colored agarwood believed to contain a greater abundance of resin.[6]

3.3 UPLC-MS-based untargeted metabolomics study

3.3.1 Identification of chemical composition. A total of 89 chromones were tentatively identified from the 24 batches of agarwood samples with different specifications (Fig. 5A), including 18 tetrahydro-2-(2-phenylethyl)chromones (THPECs), 33 2-(2-phenylethyl)chromones of the flindersia type (FTPECs), 5 epoxy-2-(2-phenylethyl)chromones (EPECs), 5 diepoxy-2-(2-phenylethyl)chromones (DEPECs), and 28 dimeric 2-(2-phenylethyl)chromones (BI). The identification information is listed in Table S1. The mass spectrometric fragmentation patterns of all identified component types were consistent with those reported in the literature.[15–19]

Tetrahydro-2-(2-phenylethyl)chromones (THPECs), 2-(2-phenylethyl)chromones of the Flindersia type (FTPECs), epoxy-(2-phenylethyl)chromones (EPECs), and diepoxy-(2-phenylethyl) chromones (DEPECs) are 2-(2-phenylethyl)chromone (PECs) monomers with four different skeletons[20] (Fig. 5B). Two chromone monomers are connected by bicyclic, O-linked, or C-linked groups to form PEC dimers.[16] The results of this study demonstrated a relatively high proportion of FTPECs among the identified components in agarwood, whereas DEPECs and EPECs were present in lower quantities. Jinling Yang,[21] through compositional analysis of agarwood with different formation periods, found that the relative contents of DEPECs and EPECs

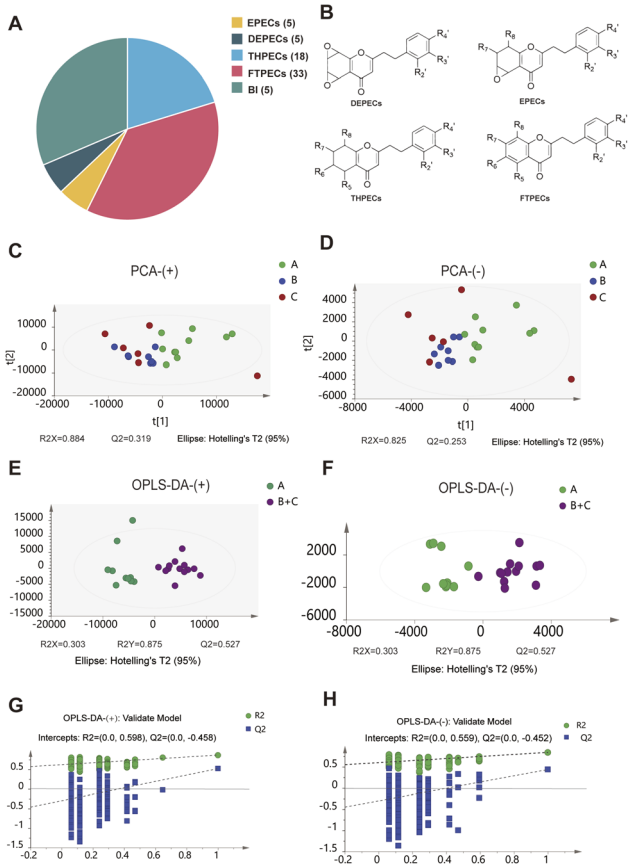

Fig. 5 Results of the untargeted metabolomics analysis. (A) proportional distribution of different chromone types identified in agarwood; (B) chemical structures of the different chromone types; (C) and (D) PCA score plots from the positive and negative ion modes, respectively; (E) and (F) OPLS-DA score plots from the positive and negative ion modes, respectively; (G) and (H) permutation test plots of the OPLS-DA models from the positive and negative ion modes, respectively. (Group A: agarwood samples with density of 0.4–0.7; Group B: density of 0.7–1.0; Group C: density > 1.0).

gradually decreased with increasing formation time, whereas the relative levels of THPECs and FTPECs showed an upward trend. Wei Li[22] proposed that DEPECs serve as precursor substances, EPECs and THPECs act as intermediates, and FTPECs are the final products. Zhen Du[16] employed UHPLC-Q-Exactive Orbitrap-MS to analyze 37 batches of agarwood and observed a higher abundance of FTPECs compared to the lesser quantities of DEPECs and EPECs. These findings corroborate previous literature reports on the patterned accumulation of PECs in agarwood, indicating that samples with longer formation periods tend to contain a greater number of FTPEC components.

3.3.2 Differential analysis of agarwood across density groups. Principal component analysis (PCA) is a linear dimensionality reduction technique that extracts useful information by transforming the original variables into a set of uncorrelated linear combinations. As a characterization tool, it can intuitively display the similarities and differences between target samples and reveal sample distribution trends.[23,24] To visually observe the overall differences between agarwood samples of different density groups, PCA was performed on both positive and negative ion mode data (positive ion mode: $R^2X = 0.884$, $Q^2 = 0.319$; negative ion mode: $R^2X = 0.825$, $Q^2 = 0.253$). The PCA score plots from both positive and negative ion modes (Fig. 5C and D) consistently demonstrated that Group A agarwood separated and formed a distinct cluster from the other two Groups (B and C), whereas Groups B and C exhibited an overlapping distribution. This indicates differences in the overall chemical composition between agarwood with densities below 0.7 and those above this threshold, while the chemical profiles of samples with densities between 0.7-1.0 and those exceeding 1.0 show relatively minor variations.

According to the Group Standard of the Fujian Eaglewood Association (China),[25] agarwood is graded as follows: Grade A samples have black–brown or yellow–brown color and a density greater than 1.0; Grade B samples have gray–brown or yellow–brown color and a density between 0.55 and 1.0; and Grade C samples have light gray–brown or light yellow–brown color and a density ranging from 0.43 to 0.55. This standard explicitly states that higher density corresponds to a superior grade and quality in agarwood. In this investigation, all samples from Groups B and C had densities greater than 0.7. As a result, the Fujian Eaglewood Association's grading guideline classifies all agarwood from Groups B and C in this study as medium-to-high grade. It is anticipated that the chemical composition changes between these medium-to-high grade samples are modest.

Orthogonal Projections to Latent Structures Discriminant Analysis (OPLS-DA) can filter out orthogonal variation unrelated to the metabolite classification, thereby maximizing inter-group separation and identifying differentially abundant metabolites. Based on the known results from the PCA score plot, minimal differences were observed between Group B (density 0.7–1.0) and Group C (density > 1.0), whereas distinct differences in overall chemical composition were found between agarwood with density below 0.7 and those with density above 0.7. Therefore, for subsequent analysis, Groups B and C were combined, and OPLS-DA was employed to further screen for differential ion peaks between agarwood with density less than 0.7 and those with density greater than 0.7.

The data matrix from Group A and the combined (B + C) Group was subjected to OPLS-DA to establish a classification model and identify differential components in the metabolic profiles between the two sample groups. In the OPLS-DA model, the positive ion mode data yielded $R^2X = 0.303$, $R^2Y = 0.875$, and $Q^2 = 0.527$, and the negative ion mode data gave $R^2X = 0.338$, $R^2Y = 0.848$, and $Q^2 = 0.442$, indicating that the model possesses a good explanatory and predictive capability. The OPLS-DA score plot (Fig. 5E and F) revealed a clear separation between Group A and the combined (B + C) Group agarwood samples, suggesting distinct differences in their chemical composition. Furthermore, the results of the permutation tests ($n = 200$) indicated that the OPLS-DA model had no risk of overfitting (positive ion mode: $R^2 = 0.598$, $Q^2 = -0.458$; negative ion mode: $R^2 = 0.559$, $Q^2 = -0.452$) (Fig. 5H and G).

The Variable Importance in Projection (VIP) score reflects the contribution of each variable to the classification model, with

a VIP value greater than 1.0 generally considered statistically significant. Additionally, the fold change (FC) value is primarily used to describe and quantify the magnitude of variation in experimental outcomes. It provides an intuitive metric for assessing whether the change in a given variable is substantial. In this experiment, the fold change (FC) was calculated as the mean value in the combined (B + C) Group divided by the mean value in Group A, representing the relative abundance ratio of a specific ion peak between Group A and the combined (B + C) Group. An FC value greater than 1.0 indicates an increase in the (B + C) Group relative to Group A, whereas a value less than 1.0 indicates a decrease. It is important to note that the fold change itself does not provide information on whether the observed variation is statistically significant. The *p*-value is primarily employed to assess the reliability or authenticity of experimental results. Generally, a *p*-value less than 0.05 is considered statistically significant. Therefore, in this experiment, using the criteria of $p < 0.05$, VIP > 1, and fold change (FC) < 0.5 or FC > 2.0, a total of 358 and 352 differential ion peaks were obtained from the positive and negative ion modes, respectively. These differential ion peaks were subsequently identified by comparing their retention times, high-resolution MS data, and fragmentation patterns with those of available reference standards or relevant literature. Ultimately, 19 differential components were successfully identified between Group A (density < 0.7) and the combined (B + C) Group (density > 0.7) (Table S2).

In total, 19 differential components were identified, comprising 8 FTPECs and 11 dimeric chromones (BI). Interestingly, all 8 FTPECs exhibited fold change (FC) values less than 0.5, whereas all 11 dimeric chromones showed FC values greater than 2.0 (Table S2). For isomers, they share an identical core scaffold but differ in their structural configuration or the position of substituents. Among the 19 differential ion peaks identified in this study, there were two peaks at *m*/*z* 693, three at *m*/*z* 675, two at *m*/*z* 267, three at *m*/*z* 625, and two at *m*/*z* 281. These differential ion peaks sharing the same mass-to-charge ratio are likely to be isomers. The putative structures of these differential ion peaks are illustrated in Fig. 6.

The peak areas of these 19 differential components across the 24 batches of agarwood were extracted, normalized *via* Z-score normalization, and used to construct a heatmap for visualizing their relative abundance relationships among different batches (Fig. 6). The results revealed that agarwood with lower density was enriched with chromone monomers, while samples with higher density contained relatively higher levels of chromone dimers.

Non-targeted metabolomic analysis in this study identified 19 differential components ($p < 0.05$, fold change > 2 or < 0.5) between low-density (<0.7) and high-density (>0.7) agarwood samples. The results revealed that the high-density group was enriched with chromone dimers, whereas the content of chromone monomers was higher in the low-density group compared to the high-density group. Studies have shown that chromones accumulate with increasing resin content in agarwood, a process accompanied by the formation and transformation of different chromone types.[26] Compared to chromone monomers, chromone dimers possess a more

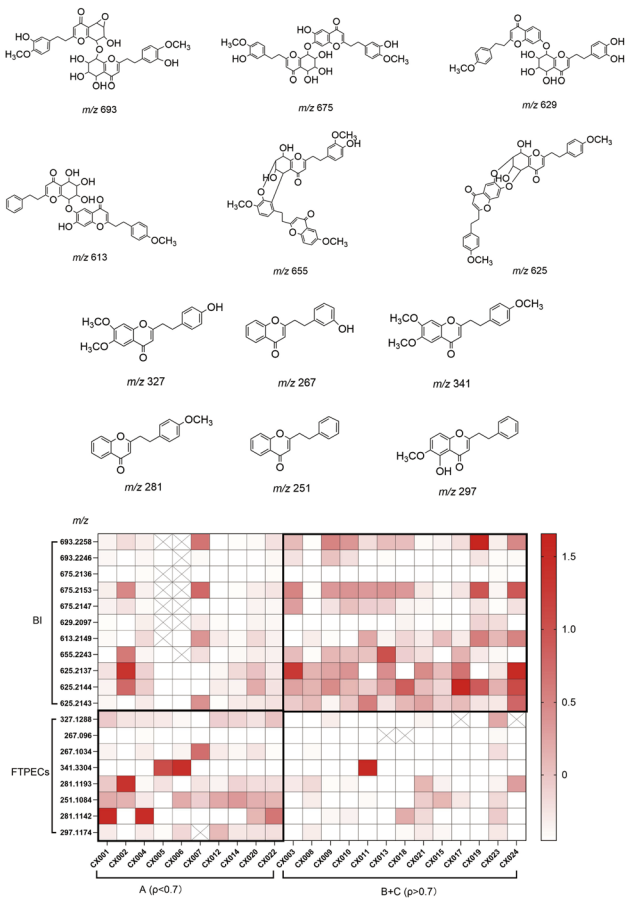

Fig. 6 Structures of differential ion peaks and their heatmap across agarwood samples.

complex structure. It is thus inferred that chromone dimers may serve as a key chemical indicator for longer formation periods and a higher degree of resinification in agarwood. In comparison to chromone monomers, chromone dimers are characterized by a larger molecular mass. This property is inferred to enable the formation of denser resinous deposits in the cellular cavities of the wood, thereby elevating the resin density. Moreover, the more elaborate conjugated system or higher oxidation level inherent to dimers augments their absorption of visible light, leading to a darkening of the resin. Consequently, these physicochemical attributes establish a scientific rationale for the observed correlation between higher density and darker coloration in agarwood. Therefore, the agarwood formation process can be summarized as follows: with prolonged resin-formation time and increased resinification, chromones undergo transformation and accumulation from monomers to dimers. The higher molecular weight and complex structure of dimers collectively contribute to increased density (sinkability) and color deepening, thereby providing a scientific explanation for the traditional empirical criterion that "sinkable and dark-colored agarwood is superior.

Further observation of the dimeric chromone structures revealed that they are all composed of one THPEC and one FTPEC unit, and each contains methoxy (–OCH_3) groups.

Studies have reported that some PECs release low molecular weight aromatic compounds upon heating, which are key components responsible for the characteristic fragrance emitted when agarwood is burned.[27] It is hypothesized that when agarwood is heated to a certain temperature, these dimeric chromones undergo cleavage and decomposition, generating a greater quantity of low-molecular-weight aromatic compounds. This process enriches the aroma profile of agarwood, making it more complex, multifaceted, and layered. Furthermore, due to their high molecular weight and low volatility, these dimeric chromones do not immediately volatilize during combustion. Instead, they breakdown gradually and constantly, releasing aromatic molecules over time, substantially increasing the duration of the distinctive agarwood fragrance. Additionally, numerous studies have reported that dimeric chromones possess various pharmacological activities, including anti-inflammatory, anticancer, and melanogenesis-inhibitory effects.[28–30] As a result, whereas dimeric chromones are not the most volatile constituents, they are expected to have a significant influence in defining both the commercial value and sensory properties of agarwood.

3.4 Quantitation of differential chromones

In the aforementioned experiments, 19 differential chromones were screened by comparing Group A (density < 0.7) against the combined Groups B and C (density > 0.7). Analysis of the fold change values revealed a lower abundance of chromone monomers in the higher density groups (B + C) compared to Group A. To validate these findings, four commercially available chromone reference standards were selected from the 19 differential components for absolute quantification: 2-(2-phenylethyl)chromone, 2-[(4-methoxyphenyl)ethyl]chromone, 6-methoxy-2-(2-phenylethyl)chromone, and 6,7-dimethoxy-2-[2-(4-hydroxyphenyl)ethyl]chromone.

The four analytes demonstrated excellent linear relationships between the measured mass concentration and peak area across their respective concentration ranges, with all correlation coefficients (r) greater than 0.9997. Precision results showed that the relative standard deviations (RSDs) for the four compounds were all below 3.83%. Stability testing indicated RSDs below 3.73% for all four compounds. Repeatability results confirmed RSDs under 6.04% for all analytes. Recovery tests demonstrated mean recovery rates ranging from 100.19% to 101.55% with RSDs below 4.92% (Table S3).

The 24 batches of agarwood samples were processed to prepare test solutions (each prepared in triplicate) and injected for analysis. The content of the four target components in each agarwood sample was calculated based on the established linear relationships described above. As shown in Fig. 7, the content of 2-(2-phenylethyl)chromone was significantly higher in Group A than in the combined (B + C) groups ($p < 0.05$). Although the other three components showed no statistically significant differences between Group A and the combined (B + C) groups, visual observation of the overall data suggests that their contents in Group A tended to be higher than those in the (B + C) groups. Furthermore, the total content of the four components was compared, revealing a significantly higher level in Group A ($p < 0.05$). This result is consistent with our earlier finding regarding the fold change of differential components, confirming that chromone monomers are more abundant in the low-density Group A agarwood than in the (B + C) groups.

Based on the traditional criterion of sinkability, this study conducted a compositional analysis of agarwood with different sinking properties. The results revealed that the four quantified components did not show higher levels in the traditionally recognized high-quality sinking agarwood. Furthermore, the sum of the contents of 2-(2-phenylethyl)chromone and 2-[2-(4-methoxyphenyl)ethyl]chromone is often used as a reference index in current Chinese agarwood grading standards.[31,32] Comparative analysis showed that the sum of these two chromones was significantly higher in the low-density Group A than in the combined (B + C) groups ($p < 0.05$). In a study by Fu Yuejin[12] comparing wild Chi-Nan agarwood, wild agarwood, and cultivated agarwood, the sum of the relative contents of 2-[2-(4-methoxyphenyl)ethyl]chromone and 2-(2-phenylethyl) chromone in cultivated and wild agarwood was significantly lower than that in wild Chi-Nan agarwood. This indicates that these two chromones are characteristic components of Chi-Nan agarwood. Therefore, the quality grading of agarwood should not rely solely on a single component or the sum of a few components as indicators. Both the Chinese Forestry Standard (LY/T 3223-2020) and the Hainan Local Standard (DB46/T 422-2017) for agarwood quality grading have incorporated the ethanol extract content as an additional reference index, besides considering the sum of the relative contents of 2-(2-phenylethyl)chromone and 2-[2-(4-methoxyphenyl)ethyl] chromone.[31,32] However, the quality of agarwood is determined

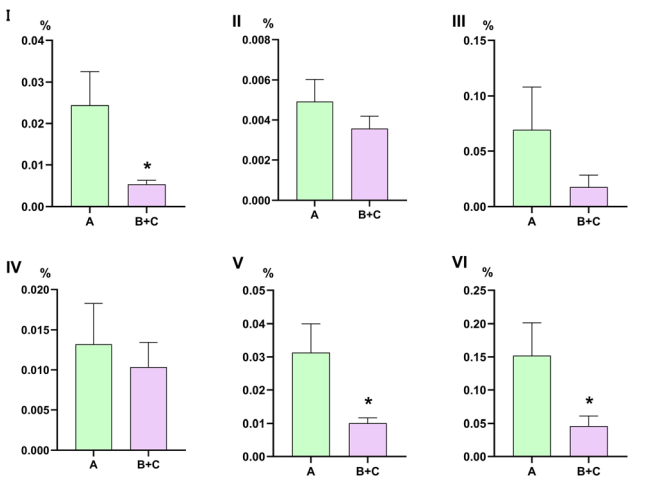

Fig. 7 Histograms showing the contents of the four target components in Group A *versus* the combined (B + C) groups. (I) 2-(2-phenylethyl)chromone; (II) 2-[(4-methoxyphenyl)ethyl]chromone; (III) 6-methoxy-2-(2-phenylethyl)chromone; (IV) 6,7-dimethoxy-2-[2-(4-hydroxyphenyl)ethyl]chromone; (V) combined content of 2-(2-phenylethyl)chromone and 2-[2-(4-methoxyphenyl)ethyl]chromone; (VI) total content of all four components. The asterisk (*) indicates statistical significance at $p < 0.05$.

by multiple factors. A comprehensive quality evaluation should integrate physical characteristics (such as sinkability and color), resin content, and chemical composition.

4 Conclusions

This study systematically validates the scientific rationale behind the traditional "sinkability test" for agarwood from a physicochemical perspective. Through an integrated investigation of sinkability, ethanol extract content, density, color, and chemical composition, we confirmed that sinkable agarwood with higher density exhibits darker coloration. For the first time, this research clearly established that high-density agarwood is enriched with high-molecular-weight components (dimeric chromones), thereby substantiating the scientific basis for the ancient standard that prioritized "sinking ability and dark color" as markers of superior quality. These findings provide a crucial data foundation for future quality grading of agarwood based on comprehensive trait indices, chemical composition, and biological activity.

Author contributions

Yanan Yuan: methodology, investigation, data curation, conceptualization, writing – review and editing. Mengyuan Yang: writing – original draft, data curation. Yujiao Zhao: experimental design, data interpretation, manuscript refinement. Zhidong Qiu: writing – review and editing, conceptualization. All authors have read and agreed to the published version of the manuscript.

Conflicts of interest

There are no conflicts to declare.

Data availability

The data that support the findings of this study are included in the supplementary information (SI) of this article. Supplementary information: one figure and three tables: Fig. S1 shows records of agarwood in China Ancient Books. Table S1 lists 89 chromones preliminarily identified from 24 batches of agarwood samples with different specifications. Table S2 shows 19 differential components between Group A and Group (B + C). Table S3 presents detailed method validation results. See DOI: https://doi.org/10.1039/d5ra08081a.

Acknowledgements

This research work was supported by the project for the National Key Research and Development Program of China (2022YFC3500900, 2022YFC3500902), the CACMS Innovation Fund (CI2024E001), the Major Increase and Reduction Project at the Central Level (2060302), and the Innovation Team and Talents Cultivation Program of National Administration of Traditional Chinese Medicine (ZYYCXTD-C-202409).

References

1 Aquilaria sinensis (Lour.) Spreng, *National Southern Medicine Gene Bank*, 2016, https://genebanker.org/retrieveshow.aspx?id=134, accessed October 2025.
2 R. Das, P. S. Naziz and S. Sen, *Science*, 2022, 46–47, https://www.researchgate.net/publication/373769524_The_Fragrance_of_Agarwood.
3 C. C. Fu, B. X. Huang, X. H. Zhang, J. L. Zhou, S. Y. Mao, T. P. Fan, J. H. Zhang, S. S. Wang, M. X. Chen and F. Y. Zhu, *J. Agric. Food Chem.*, 2025, **73**(26), 16049–16063, DOI: 10.1021/acs.jafc.5c02632.
4 M. Ren, X. L. Ren, X. Y Wang and Y. M. Yang, *Proc. Natl. Acad. Sci. U. S. A.*, 2022, **119**(21), e2112724119, DOI: 10.1073/pnas.2112724119.
5 Y. Y. Liu, J. H. Wei, Z. H. Gao, Z. Zhang and J. C. Lyu, *Chin. Herb. Med.*, 2017, **9**(1), 22–30, DOI: 10.1016/S1674-6384(17)60072-8.
6 R. Mohamed and S. Y. Lee, *Keeping up Appearances: Agarwood Grades and Quality, Agarwood: Science behind the Fragrance*, Singapore, Springer Singapore, 2016, pp. 149–167, DOI: 10.1007/978-981-10-0833-7_10.
7 M. Li, Z. Hong, S. J. Wang, D. P. Xu, Z. N. Yang, Z. H. Li, H. Z. Hu and S. X. Li, *Molecules*, 2025, **30**(2), 352, DOI: 10.3390/molecules30020352.
8 W. L. Wu, X. Y. Jiang, L. Y. Jiang, I. Wilson, F. J. Shao and D. Y. Qiu, *Plants*, 2025, **14**(7), 1012, DOI: 10.3390/plants14071012.
9 National Pharmacopoeia Commission, *Pharmacopoeia of the People's Republic of China, Beijing*, China Medical Science and Technology Press, 2020.
10 M. Yu, Y. Y. Liu, J. Feng, D. L. Chen, Y. Yang, P. W. Liu, Z. X. Yu and J. H. Wei, *Int. J. Environ. Anal. Chem.*, 2021, **2021**(1), 5593730, DOI: 10.1155/2021/5593730.
11 W. T. Lin, L. F. Liu, B. Li, X. Huang and Y. L. Liang, *Mod. Chin. Med.*, 2023, **25**(10), 2246–2254, DOI: 10.13313/j.issn.1673-4890.20221128005.
12 Y. J. Fu, L. N. Tang, Y. Chen, S. Yang, D. Y. Jia and G. Y. Li, *China Forest Products Industry*, 2020, vol. 57, 10, pp. 26–30, DOI: 10.19531/j.issn1001-5299.202010006.
13 S. T. Chen and Y. K. Rao, *Med. Tradic.*, 2022, **3**(1), 1–71, DOI: 10.35702/Trad.10008.
14 C. C. Fu, B. X. Huang, S. S. Wang, Y. C. Song, D. Metok, Y. X. Tan, T. P. Fan, A. R. Fernie, M. Zargar, Y. Wang, M. X. Chen, L. W. Yu and F. Y. Zhu, *Stress Biol.*, 2024, **4**(1), 40, DOI: 10.1007/s44154-024-00179-5.
15 H. X. Huo, H. Zhang, H. T. Liu, J. L Ma, Q. Zhang, Y. F. Zhao, J. Zheng, P. F. Tu, Y. L. Song and J. Li, *Chin. Med.*, 2025, **20**, 26, DOI: 10.1186/s13020-025-01073-6.
16 Z. Du, H. J. Wang, X. L. LI, M. Y. Dong, B. Q. Chi, Z. H. Tian, Z. G. Wang and H. Q. Jiang, *Food Chem.*, 2023, **424**, 136400, DOI: 10.1016/j.foodchem.2023.136400.
17 G. Liao, W. H. Dong, J. L. Yang, L. Wei, J. Wang, W. L. Mei and H. F. Dai, *Molecules*, 2018, **23**(6), 1261, DOI: 10.3390/molecules23061261.

18 X. F. Yang, W. L. Mei, W. Li, C. H. Pang, W. H. Dong, Y. B. Pan and Q. Zhang, *Chin. J. Top. Crops*, 2023, **44**(9), 1889–1900, DOI: 10.3969/j.issn.1000-2561.2023.09.017.

19 M. Y. Yang, Y. Y. Yuan, J. F. Wei, Y. F. Pei, Y. F. Niu, Y. F. Zhao, X. Y. Kong and Z. J. Zhang, *Pharmaceuticals*, 2025, **18**(4), 510, DOI: 10.3390/ph18040510.

20 W. Li, H. Q. Chen, H. Wang, W. L. Mei and H. F. Dai, *Nat. Prod. Rep.*, 2021, **38**(3), 528–565, DOI: 10.1039/d0np00042f.

21 J. L. Yang, W. H. Dong, F. D. Kong, G. Liao, J. Wang, W. L. Mei and H. F. Dai, *Molecules*, 2016, **21**(7), 911, DOI: 10.3390/molecules21070911.

22 W. Li, C. H. Cai, W. H. Dong, Z. K. Guo, H. Wang, W. L. Mei and H. F. Dai, *Fitoterapia*, 2014, **98**, 117–123, DOI: 10.1016/j.fitote.2014.07.011.

23 L. M. Qi, J. Q. Li, H. G. Liu, T. Li and Y. Z. Wang, *Food Funct.*, 2018, **9**(11), 5903–5911, DOI: 10.1039/c8fo01376d.

24 G. Toscano, Å. Rinnan, A. Pizzi and M. Mancini, *Energy Fuels*, 2017, **31**(3), 2814–2821, DOI: 10.1021/acs.energyfuels.6b02421.

25 FuJian Eaglewood Association. *T/FJEA 001—2017, Grade Classification for Natural Agarwood*, Fujian, China, 2017.

26 Y. Y. Sun, M. R. Wang, M. Yu, J. Feng, J. H. Wei and Y. Y. Liu, *Front. Plant Sci.*, 2024, **15**, 1437105, DOI: 10.3389/fpls.2024.1437105.

27 T. T. Yan, Z. K. Hu, Y. Chen, S. Yang, P. Zhang, Z. Hong and G. Y. Li, *Ind. Crops Prod.*, 2023, **194**, 116185, DOI: 10.1016/j.indcrop.2022.116185.

28 H. X. Huo, Z. X. Zhu, Y. L. Song, S. P. Shi, J. Sun, Y. F. Zhao, J. Zheng, D. Ferreira, J. K. Zjawiony, P. F. Tu and J. Li, *J. Nat. Prod.*, 2017, **81**(3), 543–553, DOI: 10.1021/acs.jnatprod.7b00919.

29 L. Y. Chen, W. L. Mei, L. Yang, F. Wu, C. H. Cai, J. Z. Yuan, H. Q. Chen and H. F. Dai, *Ind. Crops Prod.*, 2024, **222**, 120147, DOI: 10.1016/j.indcrop.2024.120147.

30 A. Gaspar, E. M. P. J. Garrido, F. Borges and J. M. P. J. Garrido, *ACS Omega*, 2024, **9**(20), 21706–21726, DOI: 10.1021/acsomega.4c00771.

31 National Forestry and Grassland Administration, *LY/T 3223-2020, Quality Grading of Agarwood*, Beijing, Standards Press of China, 2021.

32 Hainan Provincial Bureau of Quality and Technology Supervision, *DB46/T 422-2017, Agarwood quality grades*, Haikou, Hainan Provincial Bureau of Quality and Technology Supervision, 2017, https://amr.hainan.gov.cn/zw/dfbz/201902/t20190213_2311523.html.